International Journal on Advanced Science Engineering Information Technology

Vol.8 (2018) No. 3
ISSN: 2088-5334

Oil-Palm Plantation Identification from Satellite Images Using Google Earth Engine

Supattra Puttinaovarat[#], Paramate Horkaew[*]

[#]*Faculty of Science and Industrial Technology, Prince of Songkla University, Surat Thani Campus, Surat Thani, Thailand*
E-mail: supattra.p@psu.ac.th

[*] *School of Computer Engineering, Institute of Engineering, Suranaree University of Technology, Nakhon Ratchasima, Thailand*
E-mail: phorkaew@sut.ac.th

***Abstract*— Oil-palm plantation is a crucial determinant for land-use planning and agricultural studies. Remote sensing techniques have elevated limitations of the on-site survey as computerized imaging is much efficient and economical. This paper presents a ubiquitous application of Gabor analysis for extracting oil-palm plantation from satellite images. The proposed system was built on the cloud-based Google Earth Engine. Herein, THEOS images were convoluted with Gabor kernels, and both K-Means and SVM then learned their responses for comparison. Experimental results showed that SVM could better identify the plantation areas with precision, recall, and accuracy of 92.98%, 88.96%, and 94.24% respectively.**

***Keywords*— oil-palm plantation; texture analysis; Gabor wavelet; Google Earth Engine (GEE)**

I. INTRODUCTION

Oil-palm is an essential industrial crop of many South East Asia countries, especially those in the Malay Peninsula such as Malaysia and parts of Thailand [1]. Certain Thai cities, in particular, i.e., Krabi, Surat Thani, Chumphon, Satun, and Trang are the most suitable for planting the crop. Also, oil-palm is a low-cost and low-maintenance harvest, grown for making biofuel [2], as an alternative source of energy in the verge of drastic fossil-oil scarcity. A principal disadvantage of oil-palm, nonetheless, is that it consumes water significantly deeper and more than many other plants. Harvesting thus calls for a great deal of water resource [3]. It is therefore of state and public interests that the oil-palm plantation and its extents should be appropriately planned and regularized, in order not to cause adverse effects on coexisting food crops and to make the most of irrigation and land utilization. Determining renewable energy plants as well as oil and gas logistics could also greatly benefit from the well-planned planting policy.

Until recently, acquiring information on the oil-palm plantation had been troublesome as it involved a large of group of human resource, conducting geographical survey that is not only time consuming but also cost ineffective. Furthermore, prevalent tropical diseases, as well as climate and terrain constraints, had in many occasions, prohibited human access to some areas.

With the recent progress in Remote Sensing (RS), satellite images have often been employed in classifying agricultural areas, including palm and other industrial crops. Interpreting those areas visually by a human observer requires empirical knowledge and expertise on appearances and discriminative characteristics of land covers. The scheme is also tedious and time-consuming for any reasonably large region. Moreover, subjective interpretation is typically prone to intra and inter-observer variability. Automated computerized analysis, on the other hand, can elevate such impediments. The latter operates on various types of satellite images, e.g., those with moderate or high resolution and those with a single intensity or multi-spectral values. Identification of oil-palm plantation found in existing literature [4]–[7] can be categorized into three major groups, which are classifications based on individual pixels, calculated indices and local pattern or texture analysis. Once either of these attributes opted, it then generally served as an input to any of established machine learning frameworks (supervised and unsupervised), e.g., Support Vector Machine (SVM) [4], [5], Artificial Neural Network (ANN) [4], K-Mean Clustering and Maximum Likelihood Classification (MLC) [5]. Despite its simplicity, classification based on pixel values was restricted to a given data set and as such inapplicable for an extension to other areas and imaging modalities [4], [5]. Also, values training dataset should be carefully chosen so that they could adequately typify the plantation appearances.

Spectral indices customarily expressed as rational arithmetic of spectral values in relevant (light or very high radio) frequency bands, e.g., Near-Infrared (NIR) and Mid-Infrared (MIR). Oil-palm areas identification based on these indices similarly required an empirical set of thresholds. Associated values were not only dependent on areas but types of vegetation and other factors. Further, in some satellite modalities, there exists only visible light (RGB), some useful indices are thus unattainable. Alternatively, some studies suggested analysing local pixel pattern or texture. Although the technique requires substantial amount of pixels for reliable calculation and thus not suitable for low to medium resolution satellite images (e.g., Landsat), its favourable property is that, once the texture model has been established, extension to other studied areas is trivial since the textures characterizing oil-palm plantations and other land-covers remains invariable and discriminative across studied areas. Based on this principle, the most frequently adopted texture analysis is Gray-Level Co-occurrence Matrix (GLCM) [7], [8] where the texture is characterized by calculating how often pairs of the pixel with specific values and in a specified spatial relationship occur in a given image. For classifying vegetation problems, these values usually were Angular Second Moment, Intersecting Colours, Correlation, Variance, Inverse Difference Moment and Entropy. Several RS studies had reported using GLCM with relatively high accuracy when combined with other measures. Its noted shortcomings are that computing the statistics is highly computationally demanding and drop of the accuracy around and near the classes' boundary [9].

In computer vision applications, Gabor wavelet has been found successfully adopted in representing and discriminating texture images. This wavelet is expressed as a set of adaptive scale, orientation and frequency filters that emulate human visual system [10]–[12]. Compared to GLCM, Gabor is a more superior alternative as it yields significantly greater accuracy yet with much less processing time [9]. Despite a wide range of GIS and RS applications, Gabor wavelet has not yet to our knowledge been applied in oil-palm plantation identification. This paper thus presents its application in the said context by incorporating a viable supervised and unsupervised machine learning. The practical use of the proposed scheme was later demonstrated by building an oil-palm plantation identification system on top of the cloud-based Google Earth Engine (GEE) [13] so that it could operate anywhere, anytime and on any device.

This paper is organized as follow: Section II describes the image acquisitions employed in this study. It also introduces the background on texture analysis by using Gabor wavelet and on automated machine learning methods implemented on GEE and assessment criteria. Section III presents and discusses experimental results both visually and numerically, comparing two learning methods. Finally, section IV provides the concluding remarks of the proposed cloud-based RS system.

II. Materials and Method

This section describes the properties of images employed in this study as well as the theoretical backgrounds on involving techniques. In summary, textures of the oil-palm plantation were characterized using Gabor wavelet from the satellite images. Resulting Gabor responses were then divided into training and testing datasets for K-Means and SVM learnings, implemented on a GEE framework. The accuracy assessment criteria were also given herein.

A. Data Preparation

This study employed remotely sensed data acquired by the Thaichote (or THEOS) satellite at the resolution of 2 meters, depicted in Fig. 1. The Geo-Informatics and Space Technology Development Agency (GISTDA) acquired them. The information on oil-palm plantation used as a ground reference for identification accuracy assessment was obtained from the Land Development Department, Thailand. Without the loss of generalization ability, the scope of this study was focused at Surat Thani, a major industrial crop city located in the South of Thailand, and the acquisition date was 9 December 2012.

Fig. 1 Selected samples of Thaichote satellite images of oil-palm plantation

B. Gabor Texture Analysis

Gabor wavelet is defined as a linear filter of the Gaussian type with different scales and orientations, and convoluted with sinusoidal function at varying frequency. Each permutation constitutes a wavelet designating a particular pattern of local spatial variation within the captured domain . The aggregated responses calculated from a set of predefined wavelet can then be effectively used as a unique texture descriptor. Expression of the Gabor filter is given below:

$$k(x, y, \boldsymbol{\theta}, f, \boldsymbol{\sigma}) = g(x, y, \boldsymbol{\theta}, f, \boldsymbol{\sigma}) f(x, y, f) \quad (1)$$

$$g(x, y, \boldsymbol{\theta}, \boldsymbol{\sigma}) = \frac{1}{2\pi\sigma_x\sigma_y} \exp\left(-\frac{1}{2}\left(\frac{x_\theta^2}{\sigma_x^2} + \frac{y_\theta^2}{\sigma_y^2}\right)\right) \quad (2)$$

$$f(x, y, f) = \exp(2\pi i(\mu_0 x + v_0 y) \quad (3)$$

Where

$x_\theta = x\cos\theta + y\sin\theta$

$y_\theta = -x\sin\theta + y\cos\theta$

$\mu_0 x = \cos(f * x_\theta)$

$v_0 y = \sin(f * y_\theta)$

Moreover, σ_x and σ_y are the standard pixel deviations in horizontal and vertical directions, respectively.

This study accordingly created a Gabor bank consisting of filters with M scales and N directions. Each filter was then convoluted with a plantation image to produce an array of response images. In the subsequent experiment, *M* and *N* were respectively set to 3 and 8, and frequency f was $\sqrt{2}$. 24 responses were thus calculated for a given image. Figs. 2 and 3 illustrate a set of selected filters and corresponding responses respectively.

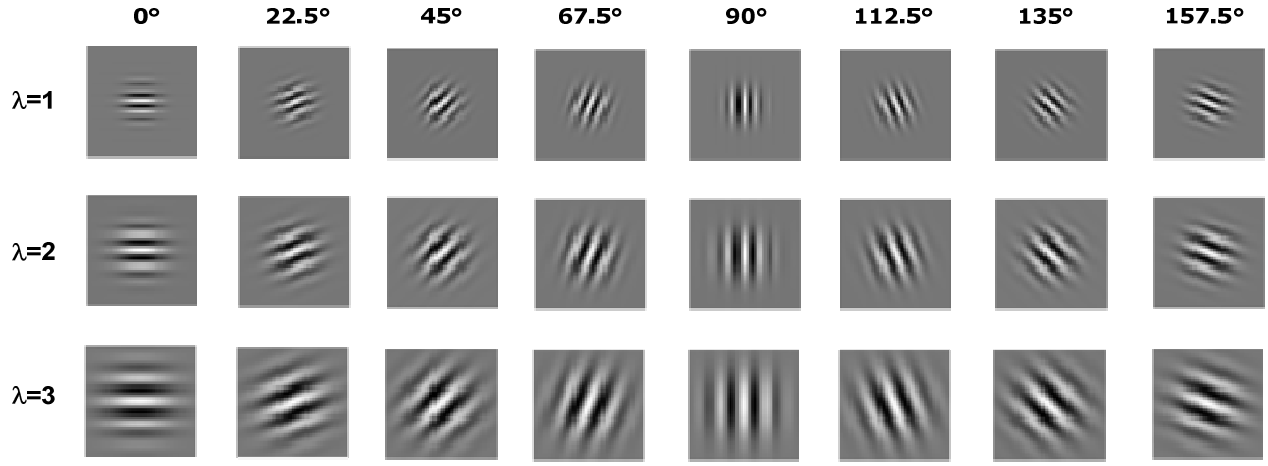

Fig. 2 Gabor filters with different scales, in pixels per cycle (vertical) and orientations (horizontal)

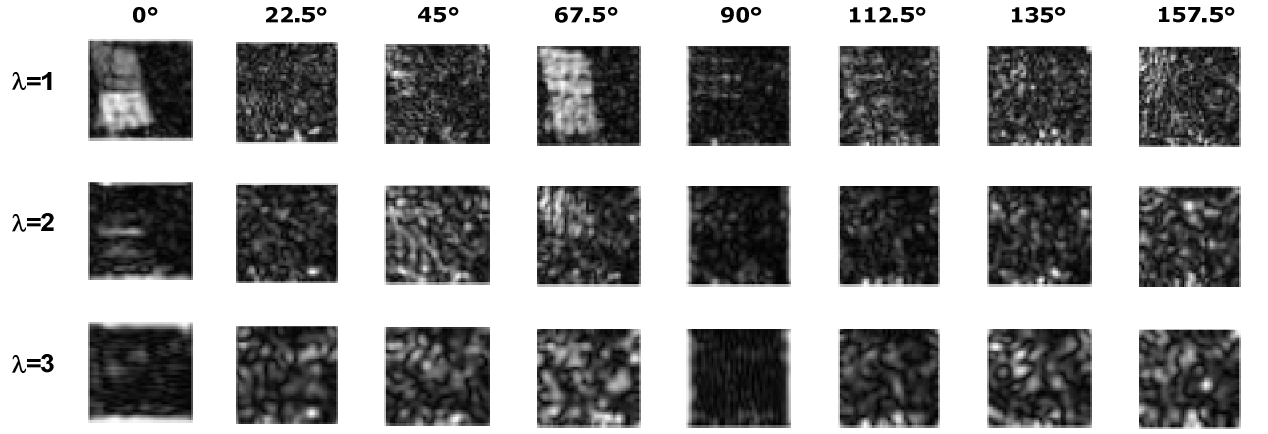

Fig. 3 Corresponding Gabor responses of the filters in Fig. 2 applied to a selected image

It is evident from the figures that, not all the kernels could be used effectively as the texture descriptors for the oil-palm plantation. This is well reflected in Fig. 3, where some responses did not pertain to any vegetation manifestation. Out of eight directions, i.e., 0˚, 22.5˚, 45˚, 67.5, 90˚, 112.5˚, 135˚ and 157.5˚, only those of 0 and 67.5 degrees could well visually describe the plantation areas. Similarly, out of 3 scales, only a unity one was sufficient for 200×200 pixels Thaichote images. Caution should; however, be observed when empirically opting any of the responses in the subsequent classifier. More specifically, should these scales and orientations were to be arbitrarily chosen, it could lead to resultant classification being subjective. Without the loss of generalization ability, this study, therefore, expanded the Gabor responses spaces with orthogonal bases, using principal component analysis (PCA). This expansion extracted the most dominant modes (or components) according to statistical variations found in the dataset. With 24 (3 by eight responses) degree of freedom (DoF), the discriminating capability of the response was assessed when the first 2, 3, 4, 5, 10, 15 and 20 components were included concerning a given classifier. This step was necessary to ensure extensibility to other areas with different plantation alignment. Consequently, each pixel consists of a multi-dimensional feature vector, i.e., the orthogonal projection of all Gabor responses on the principal components (PC). These vectors were then used for subsequent unsupervised and supervised machine learning experiments.

C. Machine Learning Classification

To assess the identification accuracies, the datasets (feature vectors obtained from section 2.(B) were divided into two classes, i.e., oil-palm plantation and other land covers, each consisted of 1000 randomly drawn pixels from 4 chosen areas in the city. Out of these pixels, 60% and 40% were used as the training and testing datasets, respectively.

In the subsequent experiments, the accuracies of K-Means and SVM methods were validated in turn against the ground reference of actual oil-palm plantations.

In the proposed scheme, the machine learnings were built on GEE framework, because it is compatible with all devices and it does not computational resource demanding. Moreover, GEE also supports various online resources of satellite images as well as uploading offline data.

On determining suitable kernels for the SVM classification, a preliminary experiment was conducted. It was found that RBF, Polynomial and Linear kernels yielded good accuracies without notable different, and a more versatile RBF thus opted in this study. Sigmoid kernel, on the other hand, failed to identify the oil-palm areas, and hence was not considered here. Due to space constraint, details of this trivial experiment was not reported in this paper. Note also that, K-Means is an unsupervised technique and hence only one set of datasets was needed for testing.

D. Accuracy Assessment

The effectiveness of oil-palm plantation identification was evaluated using statistical measures, which are precision (user accuracy), recall (producer accuracy) and total accuracy. In this study, the precision was defined as the ratio between the pixels correctly predicted as oil-palm plantation areas (true positive, TP) and those predicted as such (true and false positives, TP+FP). The recall was defined as the ratio between the pixels correctly classified, and those were in fact of the plantation areas (true positive and false negative, TP+FN). The accuracy is the proportion of the correct results among the total number of instances examined and was defined as the ratio between the pixels correctly identified as and as not the oil-palm plantation (true positive and negative, TP+TN) and the size of the test set. Finally, the Kappa coefficient measured the agreement between automated and ground reference raters, each classifying pixels in the test set into being and not being of plantation areas. The results reported in the next sections compare these statistics between those obtained by using K-Means and SVM classification.

III. Results and Discussions

Visual assessment of the resultant plantation identification as illustrated in Fig. 4, where an oil-palm plantation of the selected areas obtained by using K-Means (a) and SVM (b) are compared. Each row corresponds to when including 2, 3 and 4 PCs in the classification. It is evident that there exists an entirely fair amount of under- and over-segmented plantation pixels in K-Means cases (column a), compared to that in SVM. Fig. Five similarly depicts the classifications for four selected areas but using only 3 PCs. The resultant classification concurs with the previous observation. Closer visual inspection reveals further that K-Means classifier tended to underestimate areas with the less obvious response, hence labeling them as voids and other sporadic vegetation. These areas were, for instances, in fact, was the actual plantation cast by shadow or that were not fully-grown. SVM, however, was not so much affected by the ambiguity, probably due to its more flexible discriminating lines. Fig. 6 depicts a captured mobile screen of the proposed GEE system, demonstrating its potential online uses. Fig. 7 shows the oil-palm plantation polygon obtained by using iterative polygon fitting on an identified area.

Table 1 shows oil-palm plantation identification accuracy, when including 2, 3, 4, 5, 10, 15 and 20 PCs in the classifiers. The table lists the accuracies obtained from K-Means and SVM and their respective averages. It is noticeable that with 3 and 4 PCs included, both classifiers performed consistently well. To further determine the optimal number of PCs, Table 2 shows identification accuracies and corresponding Kappa statistics by including 2, 3 and 4 PCs. The assessment suggests that the 3 PCs cases performed best in all measures, followed by those when 4 and 2 PCs were included. Table 3 compared the statistics of identification accuracies between K-Means and SVM. It is evident that SVM classifier performed better than its counterpart, with overall accuracy, recall, precision and Kappa coefficient of 94.24%, 88.96%, 92.98% and 0.86, respectively, while K-Means classifier yielded those statistics of 89.79%, 84.63%, 84.27% and 0.76, respectively.

Finally, Fig. 8 illustrates an example of an oil-palm plantation in Surat Thani, where a) and b) are the maps of studied areas and the identified oil-palm plantation areas (black pixels). This geographical information could be valuable in the various subsequent analysis, such as determining suitable planting areas, evaluating the production capacity of an area, analyzing yield factors, deciding appropriate locations for palm oil factory, distributing hubs or purchasing yards.

Since oil palm trees are generally the same size, it is thus safe to assume that, for images at this resolution, a unit scale remains eligible for other areas. However, the orientation of oil-palm plantations varies from one area to another. Care should be taken when extending the trained PCA/SVM to other areas with different planting layouts. There exist some studies addressing an orientation invariant Gabor filter [12], which is still an area of active investigation and whose details fall out of the scope of the current study.

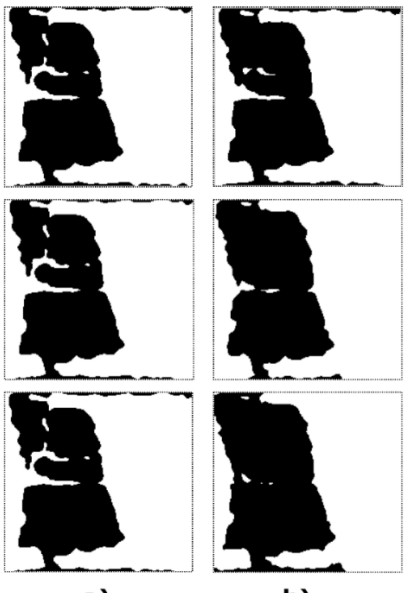

Fig. 4 Classification results for a selected area by using a) K-Means and b) SVM, taken into account different number of components (top to bottom)

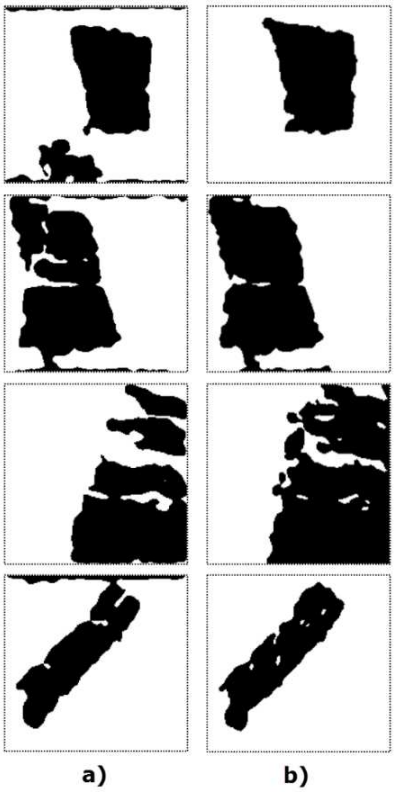

Fig. 5 Classification results for few selected areas (top to bottom) by using a) K-Means and b) SVM

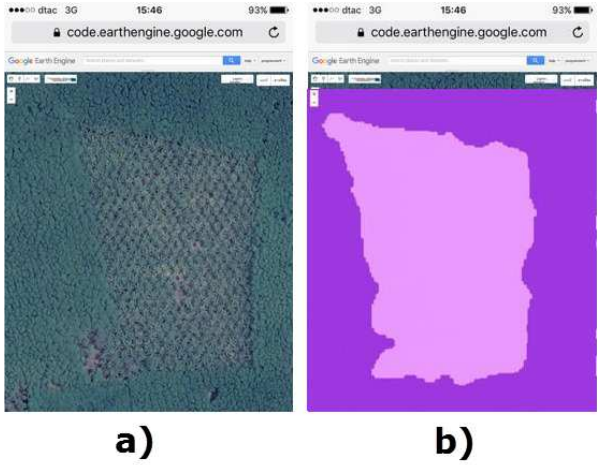

Fig. 6 Screen capture of the GEE showing a) a sample satellite image and b) corresponding oil-palm plantation extraction

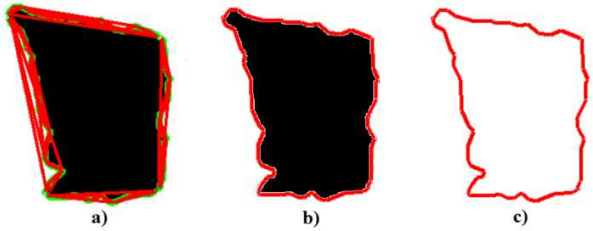

Fig. 7 Example of a polygon iteratively fitted on the identified plantation

TABLE I
AVERAGED IDENTIFICATION ACCURACY BETWEEN K-MEANS AND SVM, AT VARYING NUMBERS OF PCS INCLUDED

Image	#PC	K-Means	SVM	Average	Image	#PC	K-Means	SVM	Average
1	2	88.26	91.80	90.03	**2**	2	90.33	91.47	90.90
	3	88.48	95.65	92.07		3	90.41	94.29	**92.35**
	4	88.58	95.79	**92.19**		4	90.37	93.72	92.05
	5	89.44	94.15	91.80		5	89.97	94.07	92.02
	10	87.48	93.25	90.37		10	89.94	94.03	91.99
	15	87.49	92.82	90.16		15	89.94	93.72	91.83
	20	86.55	91.43	88.99		20	89.94	93.69	91.82
3	2	86.15	86.23	86.19	**4**	2	91.11	93.06	92.09
	3	87.02	91.07	**89.05**		3	93.23	95.94	94.59
	4	86.92	89.82	88.37		4	93.21	96.01	**94.61**
	5	85.26	88.02	86.64		5	92.13	95.98	94.06
	10	85.11	87.06	86.09		10	92.12	95.69	93.91
	15	85.11	86.92	86.02		15	92.12	92.89	92.51
	20	85.10	86.83	85.97		20	88.95	90.02	89.49

TABLE II
COMPARISONS OF IDENTIFICATION ACCURACY AND KAPPA WITH 2, 3 AND 4 PCS INCLUDED

Method/Image no.		K-means		SVM		Average	
		Accuracy	Kappa	Accuracy	Kappa	Accuracy	Kappa
Image no.1	**2 PCs**	88.26	0.70	91.80	0.77	90.03	0.74
	3 PCs	88.48	0.71	95.65	0.87	92.07	0.79
	4 PCs	**88.58**	**0.71**	**95.79**	**0.88**	**92.19**	**0.80**

Method/Image no.		K-means		SVM		Average	
		Accuracy	Kappa	Accuracy	Kappa	Accuracy	Kappa
Image no.2	2 PCs	90.33	0.79	91.47	0.82	90.90	0.81
	3 PCs	**90.41**	**0.80**	**94.29**	**0.88**	**92.35**	**0.84**
	4 PCs	90.37	0.80	93.72	0.87	92.05	0.84
Image no.3	2 PCs	86.15	0.72	86.23	0.72	86.19	0.72
	3 PCs	**87.02**	**0.74**	**91.07**	**0.82**	**89.05**	**0.78**
	4 PCs	86.92	0.74	89.82	0.80	88.37	0.77
Image no.4	2 PCs	91.11	0.74	93.06	0.80	92.09	0.77
	3 PCs	**93.23**	**0.79**	95.94	0.87	94.59	0.83
	4 PCs	93.21	0.79	**96.01**	**0.87**	**94.61**	**0.83**
Average		89.51	0.75	92.90	0.83	91.21	0.79
Average of 2 PCs		88.96	0.74	90.64	0.78	89.80	0.76
Average of 3 PCs		**89.79**	**0.76**	**94.24**	**0.86**	**92.02**	**0.81**
Average of 4 PCs		89.77	0.76	93.84	0.86	91.81	0.81

TABLE III
COMPARISON OF IDENTIFICATION STATISTICS BETWEEN K-MEAN AND SVM BASED ON 3 COMPONENTS (3 PCS)

Method/Image no.		Gabor Filter			
		Accuracy	Precision	Recall	Kappa
K-means	No.1	88.49	88.66	70.16	0.71
	No.2	90.41	85.42	89.78	0.80
	No.3	87.02	75.07	98.91	0.74
	No.4	93.23	87.94	79.67	0.79
Average.		**89.79**	**84.27**	**84.63**	**0.76**
SVM	No.1	95.65	99.67	81.75	0.87
	No.2	94.29	92.87	92.12	0.88
	No.3	91.07	91.48	90.88	0.82
	No.4	95.94	87.89	91.09	0.87
Average.		**94.24**	**92.98**	**88.96**	**0.86**

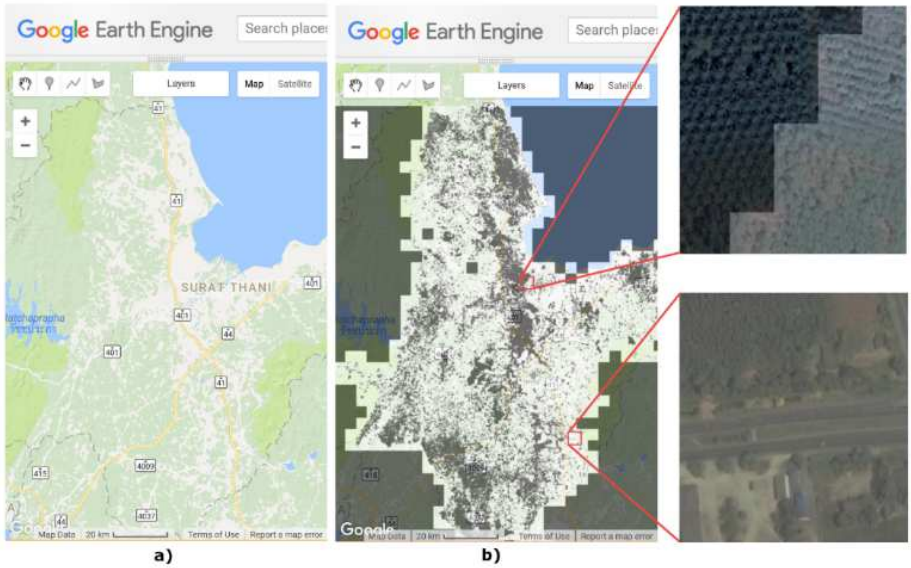

Fig. 8 Screen capture of the Google Earth Engine showing a) a sample satellite image and b) oil-palm plantation extraction of the study area. The inset figures are the zoomed in version of the plantation (top) and non-plantation (bottom) areas.

IV. Conclusions

This paper presents a cloud-based system for identifying oil-palm plantations from Thaichote (THEOS) satellite images based on underlying texture feature, characterized by the responses from a set of Gabor wavelets. The dimensionality of these features was reduced to only those dominant by using PCA and then fed into a machine learning classifier. The reported experimental results indicated that SVM classifier was superior to the K-Means counterpart. Specifically, it could correctly identify oil-palm plantations from the studied areas at 94.24% accuracy on average. The proposed system was implemented on the GEE, enabling ubiquitous accesses from interested parties. Also, GEE allows retrieval of online satellite image archives, e.g., Landsat, MODIS, Sentinel and High Resolution, that are gathered by Google as well as those uploaded by users.

The prospects for future research worth considered include orientation invariant texture analysis [14] and also taking into account other imaging sources, such as WorldView, IKONOS and QuickBird and modalities, such as Digital Terrain and Surface Models.

Acknowledgment

The authors would like to thank the Geo Informatics and Space Technology Development Agency, the Public Organization, and the Land Development Department of Thailand for providing the remotely sensed data (Thaichote) used in the preparation of the paper.

References

[1] P. Phitthayaphinant, A. Nissapa, B. Somboonsuke, and T. Eksomtramage, "An Equation of Oil Palm Plantation Areas in Thailand," *KKU Res. J.*, vol. 11, no. 1, pp. 66–76, 2012.

[2] U. Wangrakdiskul and N. Yodpijit, "Trends analysis and future of sustainable palm oil in Thailand," *King Mongkut's Univ. Technol. North Bangkok Int. J. Appl. Sci. Technol.*, vol. 8, no. 1, pp. 21–32, 2015.

[3] P. Nilsalab, S. H. Gheewala, R. Mungkung, S. R. Perret, T. Silalertruksa, and S. Bonnet, "Water demand and stress from oil palm-based biodiesel production in Thailand," *Int. J. Life Cycle Assess.*, vol. 22, no. 11, pp. 1666–1677, 2017.

[4] S. Vadivelu, A. Ahmad, and Y. H. Choo, "Remote Sensing Techniques for Oil Palm Age Classification Using Landsat-5 TM Satellite," *Sci. Int.*, vol. 26, no. 4, 2014.

[5] I. K. Nooni, A. A. Duker, I. Van Duren, L. Addae-Wireko, and E. M. Osei Jnr, "Support vector machine to map oil palm in a heterogeneous environment," *Int. J. Remote Sens.*, vol. 35, no. 13, pp. 4778–4794, 2014.

[6] S. U. Okoro, U. Schickhoff, J. Böhner, and U. A. Schneider, "A novel approach in monitoring land-cover change in the tropics: oil palm cultivation in the Niger Delta, Nigeria," *DIE ERDE–Journal Geogr. Soc. Berlin*, vol. 147, no. 1, pp. 40–52, 2016.

[7] S. Daliman, S. A. Rahman, S. A. Bakar, and I. Busu, "Segmentation of oil palm area based on GLCM-SVM and NDVI," in *Region 10 Symposium, 2014 IEEE*, 2014, pp. 645–650.

[8] S. Agustin, R. V. H. Ginardi, and H. Tjandrasa, "Identification of oil palm plantation in IKONOS images using radially averaged power spectrum values," in *Information & Communication Technology and Systems (ICTS), 2015 International Conference on*, 2015, pp. 89–94.

[9] F. Mirzapour and H. Ghassemian, "Fast GLCM and Gabor Filters for Texture Classification of Very High Resolution Remote Sensing Images," *Int. J. Inf. Commun. Technol. Res.*, vol. 7, no. 3, pp. 21–30, 2015.

[10] K. Yang, M. Li, Y. Liu, L. Cheng, Q. Huang, and Y. Chen, "River detection in remotely sensed imagery using Gabor filtering and path opening," *Remote Sens.*, vol. 7, no. 7, pp. 8779–8802, 2015.

[11] R. Xu, Y. Zeng, and Q. Liang, "A New Method for Extraction of Residential Areas from Multispectral Satellite Imagery," in *The Euro-China Conference on Intelligent Data Analysis and Applications*, 2016, pp. 93–98.

[12] D. Gabor, "Theory of communication. Part 1: The analysis of information," *J. Inst. Electr. Eng. III Radio Commun. Eng.*, vol. 93, no. 26, pp. 429–441, 1946.

[13] R. Goldblatt, W. You, G. Hanson, and A. K. Khandelwal, "Detecting the boundaries of urban areas in India: A dataset for pixel-based image classification in Google Earth Engine," *Remote Sens.*, vol. 8, no. 8, p. 634, 2016.

[14] J. Han and K.-K. Ma, "Rotation-invariant and scale-invariant Gabor features for texture image retrieval," *Image Vis. Comput.*, vol. 25, no. 9, pp. 1474–1481, 2007.